

# LINAC COHERENT LIGHT SOURCE UNDULATOR RF BPM SYSTEM \*

R. Lill, G. Waldschmidt, D. Walters, L. Morrison  
 Advanced Photon Source, Argonne National Laboratory, Argonne IL  
 S. Smith, T. Straumann, Z. Li, R. Johnson  
 Stanford Linear Accelerator Center, Sand Hill Road  
 Menlo Park, CA 94025 USA

## Abstract

The Linac Coherent Light Source (LCLS) will be the world's first x-ray free-electron laser (FEL) when it becomes operational in 2009. The LCLS is currently in the construction phase. The beam position monitor (BPM) system planned for the LCLS undulator will incorporate a high-resolution X-band cavity BPM system described in this paper. The BPM system will provide high-resolution measurements of the electron beam trajectory on a pulse-to-pulse basis and over many shots. The X-band cavity BPM size, simple fabrication, and high resolution make it an ideal choice for LCLS beam position detection. We will discuss the system specifications, design, and prototype test results.

## INTRODUCTION

The LCLS FEL will produce x-ray radiation over the 1.5-to 15-Angstrom wavelength range. To produce x-rays in this regime, the electron and photon beams within the 131-m-long undulator must be collinear to less than 10% of the transverse beam size ( $\approx 37 \mu\text{m}$  rms) over a minimum distance that is comparable to the FEL amplitude gain length ( $\approx 10$  m) in order to achieve saturation [1,2]. To establish and maintain the electron beam trajectory, a high-resolution and stable BPM system has been designed. The requirements for the system are delineated in Table 1. The beam-position resolution and stability over 1-h and 24-h periods were the major design challenges for the BPM system. Other design considerations were physical size, centering accuracy, radiation hardness, and reproducibility.

The LCLS undulator hall will house 33 undulators. The BPMs will be located in the drift space between each undulator and at the upstream end of the first undulator for a total of 34 BPMs. There are also two BPMs placed in the Linac to Undulator (LTU) transport line. The BPM system must provide stable and repeatable beam position data for both planes on a pulse-to-pulse basis for up to a 120-Hz repetition rate. The BPMs are critical for beam-based alignment and operations.

\*Work supported by U.S. Department of Energy, Office of Basic Energy Sciences, under Contract No. W-31-109-ENG-38.

Table 1. General system specifications.

Parameter	Specification	Conditions
Resolution	$< 1 \mu\text{m}$ rms	0.2– 1.0 nC
Offset Stability	$< +/- 1 \mu\text{m}$ rms	1 hour
Offset Stability	$< +/- 3 \mu\text{m}$ rms	24 hours
Dynamic Range, Position	$+/- 1\text{mm}$	10mm diameter chamber
Dynamic Range, Intensity	0.2-1 nC	PC Gun (single bunch)
Gain Error	$< +/- 10 \%$	$+/- 1\text{mm}$ range

## BPM SYSTEM OVERVIEW

The system proposed for the LCLS undulator features a high-resolution X-band cavity BPMs. Each BPM detector has a reference cavity and position cavity as shown in Fig. 1. The major sub-systems include the cavity BPM, receiver, and data acquisition components. The cavity BPM and downconverter will reside in the tunnel and the analog-to-digital converter (ADC) will be located in surface buildings.

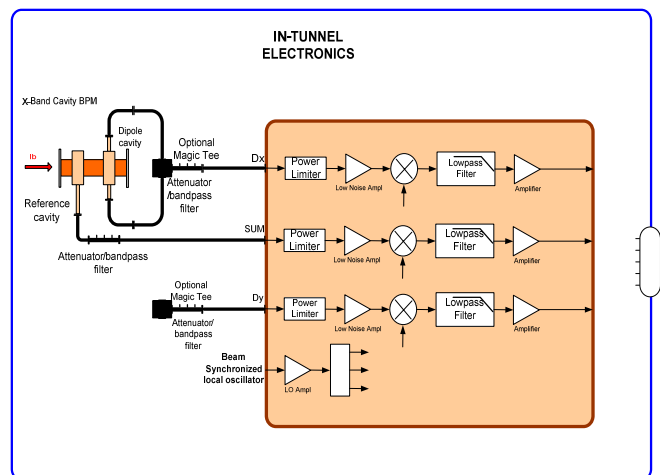


Figure 1: System block diagram.

## X-BAND CAVITY DESIGN

The simplicity of fabrication and assembly of the X-band cavity BPM due to its cylindrical geometry make it our first choice for the LCLS undulator. The cavity BPM offers the advantage of being a small, compact detector that inherently reads zero when the beam is centered. Cavity BPMs show extremely good resolution and stability. The two-cavity BPM design shown in Fig. 2 illustrates the cross section of the detector. The beam passes through the monopole reference cavity, shown on the left, which excites the  $TM_{010}$  monopole mode signal at 11.384 GHz, proportional to the beam intensity or charge. The second cavity, 37 mm downstream through the 10 mm diameter beam pipe, is the  $TM_{110}$  dipole cavity shown at the far right. The output of the dipole cavity produces a signal that is dependent on the relative beam displacement  $r/r_{fix}$  shown in equation 1 [3]. Where  $R_s/Q$  is the normalized shunt impedance of the  $TM_{110}$  mode,  $Z$  is the output line impedance,  $Q_{ext}$  is the external quality factor and  $q$  is the charge. The voltage is linearly dependent on the offset and can be scaled.

$$V_{out} = \frac{\omega_0}{2} \sqrt{\frac{Z}{Q_{ext}} \left( \frac{R_s}{Q} \right)} \frac{r}{r_{fix}} q. \quad (1)$$

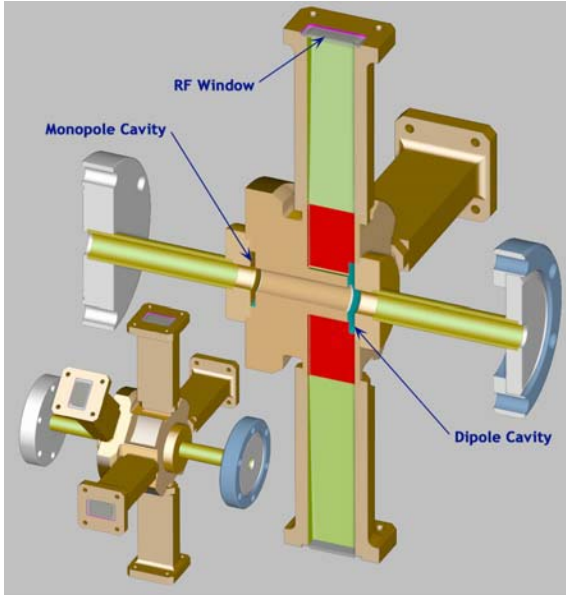


Figure 2: X-Band Cavity BPM Cross-Section.

The X-band cavity BPM inherently has the capability of resolving the beam position in the tens of nanometers, far exceeding the 1-micron resolution requirement indicated in Table 1. Equation 2 estimates the BPM thermal noise voltage output. Given the Boltzmann constant  $k$ , operating temperature  $T$  in Kelvin, impedance  $Z$  is 50 Ohms, the signal bandwidth  $B$  is about 2 MHz, and considering a system noise figure of 3 dB the minimum resolution would typically be less than 10 nm.

The single-shot resolution will be limited by other processing and data acquisition electronic noise.

$$Vn \approx \sqrt{k \times T \times Z \times B} \quad (2)$$

Horizontal and vertical position signals are generated from the two polarizations of the  $TM_{110}$  dipole mode. The polarized fields are coupled to four iris slots equally spaced around the cavity. The magnetic field of the dipole couples to the  $TM_{110}$  mode of the rectangular waveguide shown in Fig. 2. The distinctive modal patterns of the  $TM_{010}$  monopole and  $TM_{110}$  dipole modes make it possible to couple only to the dipole mode and reject the monopole mode. This selective coupling technique, pioneered by SLAC, has been incorporated in this design [4]. The iris couplers are precisely electrical discharge machined (EDM) into the solid copper block to ensure repeatable and accurate coupling. EDM provides the exceptional accuracy and repeatability that is critical for this device. This technique also ensures that the waveguide braze has little or no affect on the cavity performance from the migration of braze material. The two cavities are designed to operate at the same frequency and a small amount of tuning is provided for adjustment after brazing.

The outputs of the cavity are fed into 76-mm-long linear E-plane tapered waveguide transitions, which transform the cavity outputs (3 mm by 19.05 mm) to standard WR-75 waveguide (9.53 mm by 19.05 mm). The vacuum window shown in Fig. 3 is brazed into the WR75 waveguide flanges with a gold germanium filler alloy. The rf windows are made from glass fused onto a kovar base. The kovar is plated with nickel and then copper to facilitate brazing. The overall electrical performance of the transitions and windows together have a -20-dB return loss with less than 0.2-dB insertion loss over a 200-MHz bandwidth centered at 11.384 GHz.

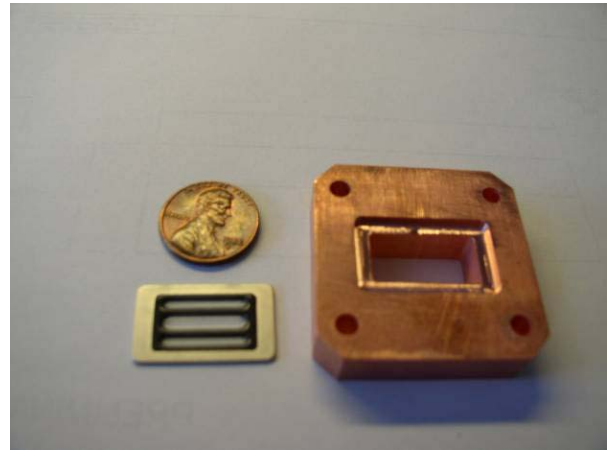


Figure 3: X-Band Cavity RF Window.

The BPM is a brazed assembly made up of the body, waveguide transitions, cavity end caps, rf windows, and end EVAC-type vacuum flanges. The 11.738-mm-radius monopole and 14.937-mm-radius dipole cavities are machined within a  $\pm 0.000/-0.015$ -mm tolerance, with a surface finish of  $0.1\ \mu\text{m}$  ( $4\ \mu\text{in Ra}$ ) or better into a single piece of oxygen-free electronic copper. The machining tolerance deviation of  $\pm 0.000/-0.015$  mm will equate to a frequency increase of 7.5 MHz, which is within the system tuning capability. The final assembly is brazed in a vacuum furnace back-filled with dry hydrogen.

To facilitate installation alignment, the outer surface of the BPM body shown in Fig. 2 is machined to be concentric to the cavity to within 0.025 mm. This surface will be used as the fiducialization reference to align the BPM during installation.

There are two waveguide outputs for each plane on the dipole cavity. The output flanges are connected directly to the flexible WR75 waveguide shown in Fig. 4 to mechanically decouple any shock or vibration from the rest of the components. The waveguide provides an ideal transmission line for the X-band signals exhibiting very low loss and excellent radiation hardness. The original design concept incorporated optional magic tee power combiners at each pair of outputs on the dipole cavity. This effectively reduces the common mode noise generated by unwanted modes by about 20 db. It is expected that full compliance to the specification can be accomplished without the use of the combiner. This would facilitate the potential for using the unused or terminated ports for future diagnostics.

Each of the three inputs to the receiver is band limited by bandpass filters. The filters provide a 20-MHz bandwidth ( $-3$  dB) centered at 11.384 GHz. The filters also provide a broadband  $-10$  dB return loss match to the cavities. Out-of-band filtering of  $-60$  db reduces unwanted modes from saturating the receiver input.

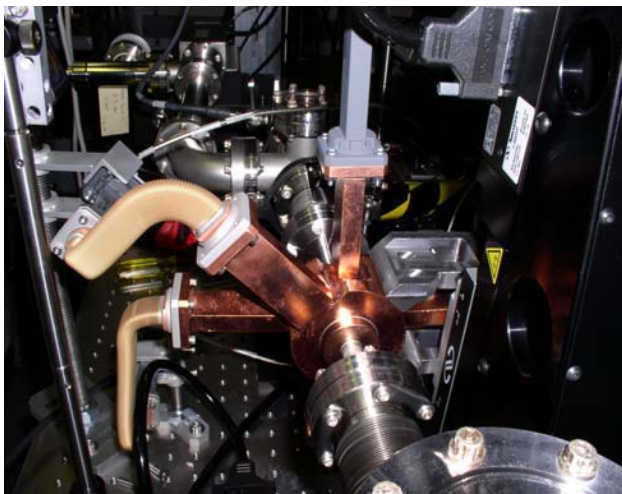


Figure 4: X-band cavity testing.

## RECEIVER DESIGN

The receiver topology used is a single-stage three-channel heterodyne receiver shown in Fig. 1. The cavity BPM X-band signals are downconverted to a 25- to 50-MHz intermediate frequency (IF) in the accelerator tunnel. The signals are first amplified in a low noise amplification (LNA) stage, then translated to a lower IF by mixing with a local oscillator (LO). The LO is a phase-locked dielectric resonator oscillator (PDRO) featuring low phase noise. One option is to lock the LO to the SLAC 119-MHz timing reference. This has the advantage of synchronizing the data with the beam. The other option would have the LO operate in a free-run mode. A single LO will drive all three channels and will be housed in the receiver chassis. The LNA is protected against high-power surges by a limiter that is rated at 50 W peak. After the X-band signals are down-converted, they are filtered and then amplified. The signals are then cabled out of the tunnel. The expected output of the receiver will be a bipolar  $\pm 1$ -volt full-scale exponentially decaying sine wave between 175-260 ns ( $Q=2000-3000$ ) in duration.

The receiver will be housed in an aluminum 3 in. high  $\times$  12 in. wide  $\times$  12 in. deep shielded enclosure. The unit will not dissipate more than 20 W and can be heat sunk. Special consideration is given to electro magnetic interference (EMI) susceptibility and emissions by using DC blocks on the inputs, EMI gaskets, feed through pins, and proper grounding. The receiver will be mounted in the tunnel below the undulator girder.

The data acquisition utilizes a commercially available ADC digitizer board. The ADC front end should have a minimum of 14-bit resolution and a sampling rate of 119 MSPS. The ADC clock will be synchronized to the frequency of the 119-MHz timing system of the SLAC linac. This will be considered the minimum requirement for the ADC and it is hoped that the performance requirement can be exceeded when the system is required.

The original plan for acquiring data for the prototype was to simply capture the exponentially decaying waveform and digitally peak detect the reference and position signals. The position and reference cavity IF signal data would then be fit to an exponential curve, with the position data being normalized to the reference.

Another processing algorithm being investigated is to digitally down-convert the IF signals. The raw digital waveform is multiplied point-by-point by a complex LO  $e^{j\omega t}$  where  $\omega$  is the IF frequency. A digital low-pass filter removes the  $2\omega$  component leaving a complex baseband signal. A quasi-Gaussian, symmetric, finite impulse response (FIR) digital filter is chosen to remove the  $2\omega$  product as well as out-of-band noise. The complex amplitude of the position signal is normalized by the reference cavity to remove bunch charge dependence (amplitude) and beam arrival time dependence (phase). Normalized phase and amplitude are converted to position via scaling and rotation by calibration data.

## PROTOTYPE RESULTS

Two X-band cavity BPMs have been prototyped and cold tested using a test fixture that precisely moves an  $\lambda/4$  E probe driven by an Hp 8510 network analyzer that excites the cavity and then measures the response. Table 2 shows the predicted and measured results of a bolted-together prototype and brazed prototype. The monopole and dipole cavities were modeled using HFSS [5]. The difference of predicted vs. the measured frequency for the  $TM_{110}$  dipole mode was less than 0.2 % for both prototypes.

Table 2: Prototype cold test results.

Parameter (500 $\mu$ m offset)	Predicted	Measured Prototype # 1 bolted end caps	Measured Prototype # 2 brazed end caps
Frequency $TM_{010}$	8.262 GHz	8.271 GHz	8.243 GHz
Coupling $TM_{010}$	-53 dB	-69 dB	-62 dB
Frequency $TM_{110}$	11.364 GHz	11.344 GHz	11.357 GHz
Coupling $TM_{110}$	-32 dB	-28 dB	-24 dB
Q (loaded) $TM_{110}$	2704	2086	2391
X/Y Isolation $TM_{110}$	-26 dB	-33 dB	-23 dB
Dipole to Monopole cavity Isolation	<-80 dB	<-85 dB	<-89 dB
Frequency $TM_{020}$	15.825 GHz	15.767 GHz	15.785 GHz
Coupling $TM_{020}$	-78 dB	-64 dB	-50 dB

The brazed prototype cavity BPM is presently installed in the Advanced Photon Source Injector Test Stand (ITS) shown in Fig. 4. The BPM is mounted on a precision 2-axis translation stage to test and calibrate the BPM. The ITS provides 1-nC single-bunch charge with bunch lengths 3-4 ps FWHM. The preliminary data shown in Table 3 indicates good correlation with the cold test and predicted values. An estimated voltage output of the dipole cavity was calculated to be 2.3 mV/ $\mu$ m/nC and the measured value was 1.22 mV/ $\mu$ m/nC. The current monitor used for this measurement has been recently recalibrated and the BPM output response will be re-measured.

Table 3. Prototype ITS test results.

Parameter	Predicted	Cold Test	ITS Test
Frequency	11.364 GHz	11.357 GHz	11.359 GHz
Loaded Q	2704	2391	2500
Isolation X/Y	-26 dB	-23 dB	-21 dB

## CONCLUSIONS

X-band cavity BPM and receiver electronics have been designed and tested for micron-level resolution for eventual installation into the LCLS. Preliminary low-power test and beam test using the ITS have produced encouraging results in validating the design for achieving the stated goals. ITS testing is scheduled to continue to obtain valuable operational experience.

The second phase of testing will involve building three new BPMs and installing them at a fixed distance from each other in order to measure single-shot trajectories. The new BPMs will incorporate changes that will facilitate a small amount of cavity tuning. The BPMs will be installed in the APS LEUTL tunnel in October 2006. The testing objective is to provide a complete compliance table for the given specification given in Table 1. Beam conditions will be similar to the expected LCLS photo cathode beam. The prototype testing should be complete by early next year, followed by the production of 34 cavity BPMs.

## ACKNOWLEDGMENTS

The authors would like to acknowledge Stephen Milton, John Carwardine, Glenn Decker, and Om Singh for many helpful discussions. The authors would also like to thank Randy Zabel for all his help with building and testing the prototypes.

## REFERENCES

- [1] R. Hettel, R. Carr, C. Field, and D. Martin, "Investigation of Beam Alignment Monitor Technologies for the LCLS FEL Undulator," BIW 98, Stanford CA, May 1998, p. 413.
- [2] P. Emma, J. Wu, "Trajectory Stability modeling and Tolerances in the LCLS," EPAC 2006, Edinburgh, Scotland, June 2006.
- [3] A. Liapine, [www.hep.ucl.ac.uk/~liapine/part\\_one\\_waveguides\\_and\\_cavities.doc](http://www.hep.ucl.ac.uk/~liapine/part_one_waveguides_and_cavities.doc)
- [4] Z. Li, R. Johnson, S. Smith, T. Naito, J. Rifkin, "Cavity BPM with Dipole-Mode-Selective Coupler," PAC 03, Portland Oregon, May 2003.
- [5] Ansoft HFSS, version 10.0, Ansoft Corporation, Pittsburgh, PA, USA, 2005.